

# ChemComm

Accepted Manuscript



This is an *Accepted Manuscript*, which has been through the Royal Society of Chemistry peer review process and has been accepted for publication.

*Accepted Manuscripts* are published online shortly after acceptance, before technical editing, formatting and proof reading. Using this free service, authors can make their results available to the community, in citable form, before we publish the edited article. We will replace this *Accepted Manuscript* with the edited and formatted *Advance Article* as soon as it is available.

You can find more information about *Accepted Manuscripts* in the [Information for Authors](#).

Please note that technical editing may introduce minor changes to the text and/or graphics, which may alter content. The journal's standard [Terms & Conditions](#) and the [Ethical guidelines](#) still apply. In no event shall the Royal Society of Chemistry be held responsible for any errors or omissions in this *Accepted Manuscript* or any consequences arising from the use of any information it contains.

## Activation of Si-H bonds across the nickel carbene bond in electron rich nickel PC<sub>carbene</sub>P pincer complexes†

Etienne A. LaPierre, Warren E. Piers, Denis M. Spasyuk and David W. Bi

Received 00th January 20xx,  
Accepted 00th January 20xx

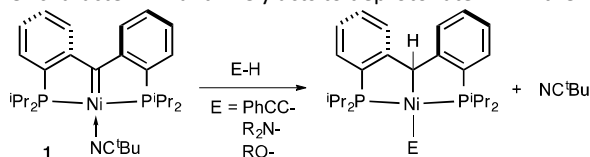
DOI: 10.1039/x0xx00000x

www.rsc.org/

**Silicon-hydrogen bonds are shown to add to a nickel carbon double bond to yield nickel  $\alpha$ -silylalkyl hydrido complexes. Kinetic and isotope labeling studies suggest that a concerted 4-centred addition across the Ni=C bond is operative rather than a mechanism involving Si-H oxidative addition. This constitutes an example of Si-H bond activation via ligand cooperativity.**

The homogeneously catalysed hydrosilylation of unsaturated functions is a commercially important process that relies on the facile activation of Si-H bonds. While mechanisms that rely on sigma bond metathesis or heterolytic hydride abstraction pathways are operative in early transition metal<sup>1</sup> and main group element catalysts,<sup>2</sup> respectively, for late metals this activation typically takes place via oxidative addition.<sup>3</sup> Activation mechanisms that involve a ligand engaging cooperatively in the Si-H bond cleavage step are less common.<sup>4-8</sup>

Recently, we described a family of nickel PC<sub>carbene</sub>P pincer complexes which rapidly added protic E-H bonds (E = RCC-, R<sub>2</sub>N- and RO-) across the anchoring C=Ni linkage such that the nucleophilic E group ends up bonded to nickel (Scheme 1).<sup>9, 10</sup> In this system, the Ni carbene adopts a nucleophilic, "Schrock-like" character<sup>11, 12</sup> and likely acts to deprotonate E-H in the

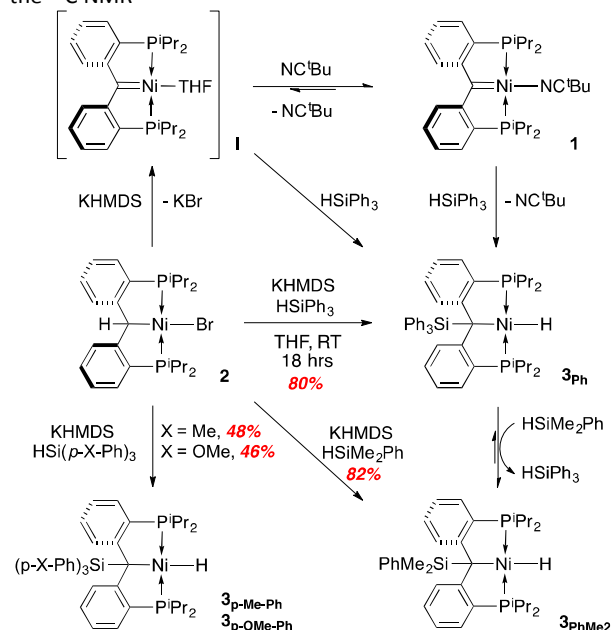


Scheme 1. Addition of protic E-H bonds to Ni=C.

<sup>a</sup> University of Calgary, Department of Chemistry, 2500 University Drive N.W., Calgary, Alberta, Canada, T2N 1N4. wpiers@ucalgary.ca

†Electronic Supplementary Information (ESI) available: Text and Figures giving further experimental and spectroscopic details, X-ray structural data for 3<sub>p-Me-Ph</sub>, 3<sub>p-OMe-Ph</sub>, 3<sub>PhMe2</sub> and 4, (CCDC 1435802-1435807) and full details on the computational work. See DOI: 10.1039/x0xx00000x

key step leading to product. We were interested in how these compounds would interact with E-H bonds in which the polarity is reversed and the hydrogen is more hydridic in character. Accordingly, we have explored the reactivity of this system with various tertiary silanes and describe evidence for direct, concerted addition of Si-H across the Ni=C bond such that the silicon is delivered to the nucleophilic carbene carbon. The tert-butyl nitrile stabilized PC<sub>carbene</sub>P complex 1<sup>9</sup> reacts with triphenylsilane in benzene or THF to yield a yellow solution of a nickel hydrido product with a characteristic upfield triplet resonance at -13.56 ppm (<sup>2</sup>J<sub>HP</sub> = 62 Hz). The disappearance of the carbene carbon signal at 110.2 ppm in the <sup>13</sup>C NMR



Scheme 2. Addition of tertiary silanes to Ni=C; synthesis of compounds 3.

spectrum for **1**, and detection of a  $^{29}\text{Si}$  signal at  $-4.2$  ppm via a  $^1\text{H}$ - $^{29}\text{Si}$  HMBC experiment suggested the  $\text{Ph}_3\text{Si}$  group is attached to anchoring carbon of the  $\text{PC}_{\text{alkyl}}\text{P}$  ligand as depicted for **3<sub>Ph</sub>** in Scheme 2. Purification of **3<sub>Ph</sub>** from these reactions was complicated by the nitrile byproduct, so a second protocol for the preparation of **3<sub>Ph</sub>** was developed, wherein the  $\text{PC}_{\text{alkyl}}\text{P}$  nickel (II) bromide **2<sup>9</sup>** was dehydrohalogenated using KHMDS in the presence of triphenylsilane. Here, the presumed THF solvated  $\text{PC}_{\text{carbene}}\text{P}$  intermediate **I** shown in Scheme 2 is rapidly trapped by the silane rather than the nitrile ligand as in the synthesis of **1**. We propose **I** as the intermediate in this process because the known compound  $(\text{PC}_{\text{alkyl}}\text{P})\text{Ni}(\text{SiMe}_3)_2$  does not form when **2** is treated with KHMDS in THF solvent;<sup>9</sup> furthermore, separately prepared amido complex does not react with silane under the conditions of this experiment. Since the preformed carbene complex **1** also engages in this reactivity, it seems likely that **I** is the key species in the formation of **3<sub>Ph</sub>**. Thus, as **I** is generated through dehydrohalogenation of **2** in THF, it reacts rapidly with the silane present to yield the observed product. By the dehydrohalogenation method, **3<sub>Ph</sub>** is easily isolated from the non-basic  $\text{HN}(\text{SiMe}_3)_2$  byproduct in 80% yield as analytically pure yellow crystals; its structure was confirmed by X-ray crystallography.

The molecular structure of **3<sub>Ph</sub>** is shown in Figure 1, along with selected metrical data. The Ni(1)-C(1) distance of  $2.043(4)\text{Å}$  is elongated by  $0.04$ - $0.06\text{Å}$  in comparison to related  $\text{PC}_{\text{alkyl}}\text{P}$  compounds<sup>9, 10</sup> due to the strong *trans* influencing hydrido donor and the steric presence of the  $\text{Ph}_3\text{Si}$  group, which also causes the phenyl group linking C(1) and P(1) to tilt  $44.2(6)^\circ$  out of the plane defined by the aryl group connecting P(2) and C(1). Although the plane of one of the phenyl rings on the silicon atom lies closely along the C(1)-Ni(1) vector, there does not

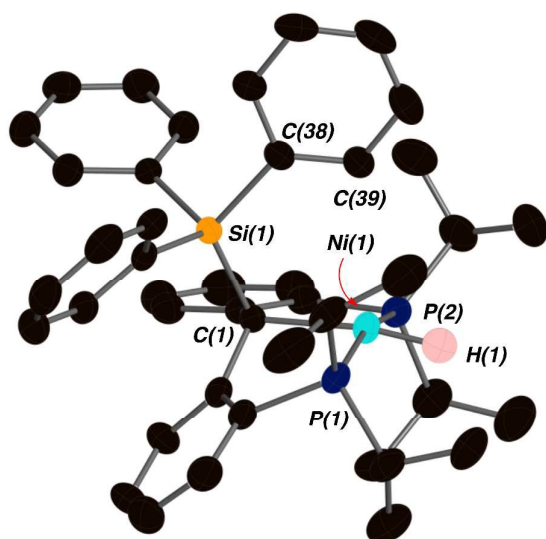


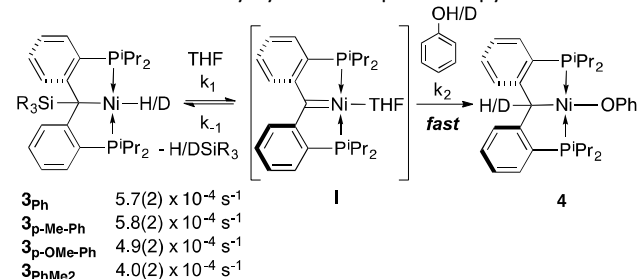
Figure 1. Molecular structure of **3<sub>Ph</sub>**. Most hydrogen atoms are omitted for clarity. Selected bond and non-bonded distances (Å): Ni(1)-C(1),  $2.043(4)$ ; Ni(1)-P(1),  $2.1344(14)$ ; Ni(1)-P(2),  $2.1079(14)$ ; Ni(1)-H(1),  $1.32(5)$ ; C(1)-Si(1),  $1.916(4)$ ; C(39)-Ni(1),  $3.051$ . Selected bond angles ( $^\circ$ ): P(1)-Ni(1)-P(2),  $163.42(5)$ ; C(1)-Ni(1)-P(1),  $89.99(12)$ ; C(1)-Ni(1)-P(2),  $89.94(12)$ ; Si(1)-C(1)-Ni(1),  $109.8(2)$ ; C(1)-Si(1)-C(38),  $116.5(2)$ .

appear to be an agostic interaction present between the C-H bond on C(39) and the Ni(1) center based on the long Ni(1)-C(39) distance of  $3.051\text{Å}$ . Furthermore, the open C(1)-Si(1)-C(38) angle of  $116.5(2)^\circ$  is suggestive of a repulsive rather than an attractive interaction.

As depicted in Scheme 2, this dehydrohalogenative protocol can be used to prepare the related derivatives **3<sub>p-Me-Ph</sub>**, **3<sub>p-OMe-Ph</sub>** and **3<sub>PhMe2</sub>** in moderate to good yields. Each was fully characterized by multinuclear NMR spectroscopy and X-ray crystallography; details can be found in the ESI (Figures S1-3). The phenyldimethylsilyl derivative **3<sub>PhMe2</sub>** was also prepared by treating **3<sub>Ph</sub>** with a moderate excess of  $\text{PhMe}_2\text{SiH}$  in THF (Scheme 2). Notably, this reaction does not take place in benzene solution, suggesting that **I** incorporates ligated THF. For these two silanes, the equilibrium lies strongly towards the less hindered **3<sub>PhMe2</sub>** derivative, but with addition of an excess of  $\text{Ph}_2\text{SiH}$  to **3<sub>PhMe2</sub>**, the equilibrium can be driven partially back towards **3<sub>Ph</sub>**. These observations are significant because they illustrate that silane addition to the nickel carbene linkage of putative **I** is reversible and thus provide a means by which the mechanism of the activation of Si-H by **I** can be probed.

Given the system of chemistry depicted in Scheme 2, there are two avenues possible for examination of this mechanism: study of the reactions of **1** with various silanes, or investigation of the loss of silane from compounds **3<sub>Si</sub>** via the trapping of **I** by another reagent. We chose the latter, since in that instance the reactivity central to Si-H bond transformation is likely rate limiting; in the reactions of **1**, loss of the nitrile ligand is rate limiting and so the key Si-H bond activation step is not probed directly. By the principle of microscopic reversibility,<sup>13</sup> the mechanism of Si-H bond activation by **I** can be inferred from details of Si-H bond formation from compounds **3**.

Accordingly, we examined the kinetic behaviour of the reactions of compounds **3<sub>Si</sub>** with an excess of phenol, which rapidly—and irreversibly<sup>9</sup>—traps the carbene intermediate **I** to form the  $(\text{PC}_{\text{alkyl}}\text{P})\text{NiOPh}$  **4** (Scheme 3). Phenolate **4** was prepared separately and fully characterized, including via X-ray crystallography (see Figure S2 in the ESI for details). It is characterized by a resonance in the  $^{31}\text{P}$  NMR spectrum at  $38.4$  ppm, distinct from those of compounds **3<sub>Si</sub>** which all resonate at around  $56$  ppm. Therefore, the conversions of **3<sub>Si</sub>** to **4** were monitored conveniently by  $^{31}\text{P}$  NMR spectroscopy.

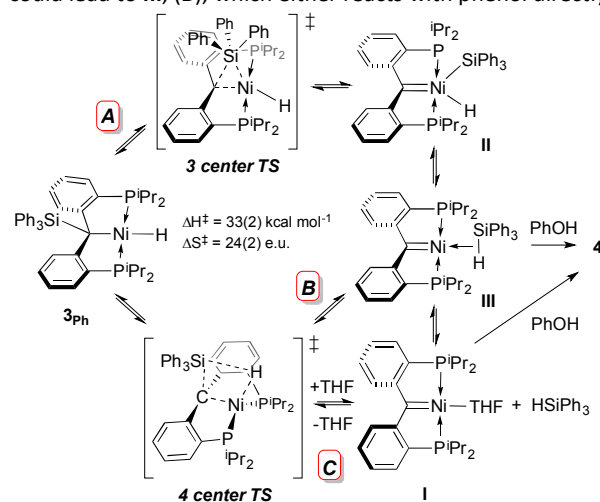


Scheme 3. Kinetics of silane elimination from compounds **3<sub>Si</sub>**.

These experiments show that conversion of compound **3<sub>Ph</sub>** to **4** is first order in  $[\mathbf{3}_{\text{Ph}}]$  (Figure S3) with a rate constant of  $5.7(2) \times 10^{-4} \text{ s}^{-1}$ . The rate of the reaction is independent of the

amount of added phenol (2 – 10 equivalents), indicating that the reaction of phenol with the product of silane loss from **3<sub>Ph</sub>** is rapid. Furthermore, the rate is not affected by the inclusion of additional excess triphenylsilane (0 – 6 equivalents), indicating that  $k_{-1}$  is also small relative to  $k_2$ . The first order rate constants, however, did vary slightly with the nature of the substitution on the silicon atom<sup>†</sup> and the rate constants are shown in Scheme 3. Two labelling experiments were conducted. In the first, the rate of conversion of **3<sub>Ph</sub>-d<sub>1</sub>** (labelled in the nickel hydride position) to **4** was followed. The label was exclusively localized in the Ph<sub>3</sub>SiD product, and an inverse KIE ( $k_H/k_D$ ) of 0.90(3) was recorded (Figure S4-5). In the second labelling experiment, the reaction was performed using C<sub>6</sub>D<sub>5</sub>OD as the trapping agent and here the label ended up exclusively in the benzylic position of the PC<sub>alkyl</sub>P ligand in **4** (Figure S6) and proteo Ph<sub>3</sub>SiH was selectively produced. Finally, an Eyring analysis of rate constants obtained for the reaction of **3<sub>Ph</sub>** with PhOH (10 equiv) at four temperatures between 50 and 80°C gave activation parameters of  $\Delta H^\ddagger = 33(2)$  kcal mol<sup>-1</sup> and  $\Delta S^\ddagger = 24(2)$  cal mol<sup>-1</sup> K<sup>-1</sup> (Figure S7).

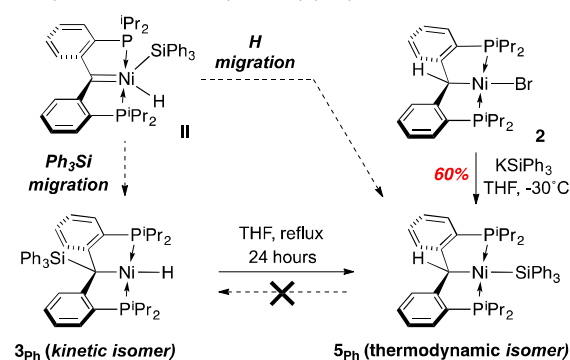
Potential mechanisms for the elimination of silane from compounds **3<sub>Si</sub>** (and therefore the reverse, activation of silane by the PC<sub>carbene</sub>PNi fragment) are shown in Scheme 4. Path **A** invokes a migration of the R<sub>3</sub>Si group from carbon to nickel via a 3-centred transition state to give the formally Ni(IV) silyl hydride **II**, which reductively eliminates silane to generate **I** (perhaps via silane complex **III**), which is trapped by phenol to give product **4**. This would imply that silane addition to **I** would occur by oxidative addition of the Si-H bond to the Ni(II) center. The other two plausible paths (**B** and **C** in Scheme 4, depending on whether or not silane complex **III** is on the path for silane elimination) proceed through direct Si-H bond formation via the 4-centred transition state depicted. Here, the geometry of the nickel centre likely distorts towards tetrahedral in order to achieve the spatial arrangement necessary for Si-H bond formation. Such a transition state could lead to **III**, (**B**), which either reacts with phenol directly or



Scheme 4. Potential mechanisms for Si-H bond formation/cleavage at (PC<sub>carbene</sub>P)Ni fragments.

dissociates silane to give **I**; alternatively, direct loss of silane gives **I** without the intermediacy of **III** (path **C**). In either of these scenarios, silicon-hydrogen bond cleavage involves nucleophilic attack by the carbene carbon on the silicon in the concerted addition of Si-H across the Ni=C bond.

Although based on the more commonly observed<sup>3</sup> Si-H oxidative addition, path **A** is unlikely for a few reasons. First, it is not entirely consistent with the kinetic data obtained (see discussion below). Second, while oxidative addition of Si-H to Ni(0) is known,<sup>14-17</sup> addition to Ni(II) to give Ni(IV) compounds is less precedented.<sup>18</sup> Third, it is not easy to understand why a species such as **II** would selectively lead to **3<sub>Ph</sub>** in the reverse reaction, since migration of the hydride ligand to the carbene carbon to form the isomeric complex **5<sub>Ph</sub>** should be competitive with Ph<sub>3</sub>Si migration (Scheme 5).<sup>8</sup> In support of this latter hypothesis, as shown in Scheme 5, the nickel silyl complex **5<sub>Ph</sub>** can be separately prepared via



Scheme 5. Separate synthesis of nickel silyl isomer **5<sub>Ph</sub>**.

treatment of **2** with *in situ* generated KSiPh<sub>3</sub> and both experiments and computations indicate that it is thermodynamically preferred over **3<sub>Ph</sub>**.

Nickel silyl<sup>14, 17, 19, 20</sup> isomer **5<sub>Ph</sub>** is characterized by a <sup>31</sup>P NMR resonance at 52.8 ppm that exhibits <sup>29</sup>Si satellites (<sup>2</sup>J<sub>P-Si</sub> =

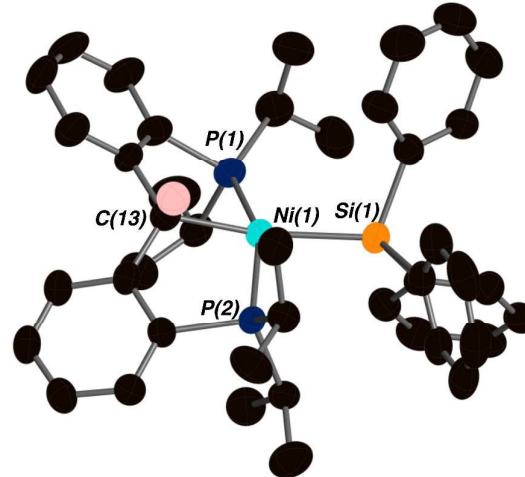


Figure 2. Molecular structure of **5<sub>Ph</sub>**. Most hydrogen atoms are omitted for clarity. Selected bond and non-bonded distances (Å): Ni(1)-C(13), 2.030(8); Ni(1)-P(1), 2.194(2); Ni(1)-P(2), 2.168(2); Ni(1)-Si(1), 2.338(2). Selected bond angles (°): P(1)-Ni(1)-P(2), 153.26(9); C(13)-Ni(1)-Si(1), 161.7(2); C(13)-Ni(1)-P(1), 84.1(2); C(13)-Ni(1)-P(2), 83.6(2); Si(1)-Ni(1)-P(1), 105.06(9); Si(1)-Ni(1)-P(2), 93.75(7).

45 Hz) and a triplet in the  $^{29}\text{Si}$  NMR spectrum at  $-0.2$  ppm ( $^2J_{\text{P-Si}} = 44$  Hz). Its molecular structure, determined by X-ray crystallography, is shown in Figure 2 and features a Ni(1)-Si(1) bond length of  $2.338(2)\text{\AA}$ . When  $\mathbf{3}_{\text{Ph}}$  is heated at reflux in THF for 24 hours, it converts to  $\mathbf{5}_{\text{Ph}}$ , albeit with about 60% decomposition (Figure S8); these other products likely arise from decomposition of THF ligated carbene **I**, which clearly forms reversibly under these conditions. In contrast, the  $^{31}\text{P}$  NMR spectrum of  $\mathbf{5}_{\text{Ph}}$  is unchanged after heating under the same conditions for several days (Figure S9). Ground state energy computations by DFT (B3LYP using the 6-31G\*\* basis set) on isomers  $\mathbf{3}_{\text{Ph}}$  and  $\mathbf{5}_{\text{Ph}}$  indicate that the silyl complex is  $7.3$  kcal mol $^{-1}$  more stable than the hydride isomer  $\mathbf{3}_{\text{Ph}}$  (Figure S10). This indicates that  $\mathbf{5}_{\text{Ph}}$  is the thermodynamic isomer, further suggesting that it should be observed in the reactions of **I** with  $\text{Ph}_3\text{SiH}$  if proceeding via an intermediate such as **II** (Scheme 4). We do not at present know much about the mechanism of the conversion of  $\mathbf{3}_{\text{Ph}}$  to  $\mathbf{5}_{\text{Ph}}$ , but it is a higher energy process than that which leads to elimination of  $\text{R}_3\text{SiH}$  from  $\mathbf{3}_{\text{Ph}}$  to yield **I**. The deuterium labelling experiments discussed above make it clear that silyl isomer  $\mathbf{5}_{\text{Ph}}$  is *not* involved in the reactions of compounds **3** with phenol; furthermore, reaction of  $\mathbf{5}_{\text{Ph}}$  with  $\text{PhOH/D}$ , while it does occur to produce **4**, is slow and the phenolic H/D label ends up on the  $\text{R}_3\text{SiH/D}$  product of this reaction (Figure S11); therefore, this reaction proceeds by a different (unknown) mechanism.

We thus conclude that the paths involving the 4-centred transition (**B/C**, Scheme 4) state are more consistent with our data, particularly path **C**. The substantially positive entropy of activation is indicative of a transition state in which the silane is well dissociated. The observed inverse KIE is also consistent with these mechanisms; in a rapid equilibrium between  $\mathbf{3}_{\text{Ph}}$  and **I** +  $\text{HSiPh}_3$ , the right hand side should be slightly favoured when deuterium is incorporated since deuterium will be preferred in the Si-H position ( $\nu_{\text{SiH}} = 2119$  cm $^{-1}$ ) than the Ni-H position ( $\nu_{\text{NiH}} = 1781$  cm $^{-1}$ ). This would increase the concentration of **I** in the deuterated isotopologue leading to overall increased rates of production of **4** in the deuterated system. The involvement of a silane complex akin to **III** is an open question, but the lack of dependence on the rate of added silane and the positive activation entropy favour direct dissociation, i.e., path **C**.

In conclusion, we propose that the reaction of silanes with the  $(\text{PC}_{\text{carbene}}\text{P})\text{Ni}(\text{THF})$  intermediate **I** occurs via concerted Si-H addition across the Ni=C linkage to produce  $\mathbf{3}_{\text{Ph}}$  as the kinetically preferred product. This mode of silane activation is rare, having been proposed on the basis of kinetic and labelling data only for highly nucleophilic Schrock type carbenes $^{21}$  where oxidative addition paths were not available. $^{22, 23}$  Here, the high energy expected for an oxidative addition pathway involving Ni(IV) directs the reactivity to the concerted path in a late metal carbene system. This reactivity attests to the high nucleophilicity associated with the Ni=C linkage in these complexes. The reversibility of the silane activation disclosed here is potentially exploitable in catalytic cycles featuring ligand cooperativity. $^{24}$

Funding for this work was provided by NSERC of Canada in the form of a Discovery Grant and an Accelerator Supplement to W.E.P. W.E.P. also thanks the Canada Research Chair secretariat for a Tier I CRC (2013–2020) and the Alexander von Humboldt Stiftung for a Research Award. The authors would like to thank Lauren Doyle for performing the ground state energy computations on compounds  $\mathbf{3}_{\text{Ph}}$  and  $\mathbf{5}_{\text{Ph}}$ .

## Notes and references

†The variation in rate constant with silane substituent does not correlate with the Hammett parameters. Rather, the rate variations appear to be related to slight changes in Si-H bond strength with changing substitution.

1. T. D. Tilley, *Acc. Chem. Res.*, 1993, **26**, 22-29.
2. W. E. Piers, A. J. V. Marwitz and L. G. Mercier, *Inorg. Chem.*, 2011, **50**, 12252-12262.
3. J. Y. Corey, *Chem. Rev.*, 2011, **111**, 863-1071.
4. S. N. MacMillan, W. Hill Harman and J. C. Peters, *Chem. Sci.*, 2014, **5**, 590-597.
5. Z. K. Sweeney, J. L. Polse, R. G. Bergman and R. A. Andersen, *Organometallics*, 1999, **18**, 5502-5510.
6. H. F. T. Klare, M. Oestreich, J.-i. Ito, H. Nishiyama, Y. Ohki and K. Tatsumi, *J. Am. Chem. Soc.*, 2011, **133**, 3312-3315.
7. M. A. Nesbit, D. L. M. Suess and J. C. Peters, *Organometallics*, 2015, **34**, 4741-4752.
8. J. Weismann and V. H. Gessner, *Chem. Commun.*, 2015, **51**, 14909-14912.
9. D. V. Gutsulyak, W. E. Piers, J. Borau-Garcia and M. Parvez, *J. Am. Chem. Soc.*, 2013, **135**, 11776-11779.
10. J. Borau-Garcia, D. V. Gutsulyak, R. J. Burford and W. E. Piers, *Dalton Trans.*, 2015, **44**, 12082-12085.
11. C. C. Comanescu and V. M. Iluc, *Organometallics*, 2014, **33**, 6059-6064.
12. C. C. Comanescu and V. M. Iluc, *Organometallics*, 2015, **34**, 4684-4692.
13. R. L. Burwell and R. G. Pearson, *J. Phys. Chem.*, 1966, **70**, 300-302.
14. V. M. Iluc and G. L. Hillhouse, *Tetrahedron*, 2006, **62**, 7577-7582.
15. R. Beck and S. A. Johnson, *Organometallics*, 2012, **31**, 3599-3609.
16. T. Steinke, C. Gemel, M. Cokoja, M. Winter and R. A. Fischer, *Angew. Chem. Int. Ed.*, 2004, **43**, 2299-2302.
17. T. Zell, T. Schaub, K. Radacki and U. Radius, *Dalton Trans.*, 2011, **40**, 1852-1854.
18. W. Chen, S. Shimada, M. Tanaka, Y. Kobayashi and K. Saigo, *J. Am. Chem. Soc.*, 2004, **126**, 8072-8073.
19. V. M. Iluc and G. L. Hillhouse, *J. Am. Chem. Soc.*, 2010, **132**, 11890-11892.
20. D. Adhikari, M. Pink and D. J. Mindiola, *Organometallics*, 2009, **28**, 2072-2077.
21. J. B. Diminnie, J. R. Blanton, H. Cai, K. T. Quisenberry and Z. Xue, *Organometallics*, 2001, **20**, 1504-1514.
22. D. H. Berry, T. S. Koloski and P. J. Carroll, *Organometallics*, 1990, **9**, 2952-2962.
23. G. Parkin, E. Bunel, B. J. Burger, M. S. Trimmer, A. Van Asselt and J. E. Bercaw, *J. Mol. Catal.*, 1987, **41**, 21-39.
24. J. R. Khusnutdinova and D. Milstein, *Angew. Chem. Int. Ed.*, 2015, **54**, 12236-12273.

Journal Name

COMMUNICATION

1

ChemComm Accepted Manuscript